A new formulation of physical surrogates of FACE A gasoline fuel based on heating and evaporation characteristics

A. E. Elwardany[1,*], S. S. Sazhin[2], H. G. Im[1]

[1]*Clean Combustion Research Centre, Division of Physical Sciences and Engineering, King Abdullah University of Science and Technology (KAUST), Thuwal 23955-6900, Saudi Arabia*

[2]*Sir Harry Ricardo Laboratories, Centre for Automotive Engineering, School of Computing, Engineering and Mathematics, University of Brighton, Brighton BN2 4GJ, United Kingdom*

Abstract

The US Department of Energy has formulated various sets of gasoline fuels, called fuels for advanced combustion engines (FACE), which are consistent in composition and properties. The analysis of heating and evaporation of FACE A gasoline fuel (paraffin-rich) is studied by replacing the 66 components with 19 components to represent this fuel. The reduction in the number of components is based on merging components from the same chemical groups and having the same chemical formula, which have very close thermophysical properties; the components with the highest initial compositions are chosen to be the representative components. Modelling of heating and evaporation of FACE A gasoline fuel and various surrogates is carried out based on the effective thermal conductivity/effective diffusivity model (ETC/ED). The model takes into account the effect of finite liquid thermal conductivity, finite liquid mass diffusivity and recirculation inside the droplets due to their non-zero velocities relative to the ambient air. Four surrogates of FACE A found in the literature are used in the analysis. These surrogates include the five component surrogate chosen for its ability to match the ignition delay time of the FACE A gasoline fuel (Surr1), the primary reference fuel surrogate (PRF84) that matches the research octane number (RON) of FACE A, the one that matches

hydrogen-to-carbon ratio (H/C), RON, density and distillation curve with FACE A (Surr2), and the one that matches the RON based on mole fraction linear blending (Surr3). It is shown that these surrogates cannot predict adequately the time evolution of surface temperatures and radii of FACE A droplets. New 'physical' surrogates with 8, 7 and 6 components (Surr4, Surr5, and Surr6) are introduced to match the evaporation characteristics of FACE A. It is found that Surr5 (7 components surrogate) can predict droplet lifetime and time evolution of surface temperature of a FACE A droplet with errors of up to 5% and 0.25%, respectively. Also, the results show that the H/C, molecular weight and RON of the new surrogates are reasonably close to those of FACE A. These results allow us to recommend that FACE A gasoline fuel can be replaced by the 7 component surrogate that matches H/C, molecular weight, and the RON of FACE A, and adequately predicts the lifetime and surface temperatures of this particular fuel droplet.

Keywords: Heating, Evaporation, Droplet, FACE gasoline fuel, Surrogate

*Corresponding author, e-mail: Ahmed.Elwardani@kaust.edu.sa, telephone: +966(0)544700974

1. Introduction

Commercial gasoline fuels used in internal combustion (IC) engines are complex mixtures of hundreds of hydrocarbon species [1], with compositions depending strongly on the origins of the fuels. This has led to a wide range in the measured performance data, making it difficult to characterise their combustion and emission behaviour at controlled engine operation conditions. This motivated the US Department of Energy to standardise the formulations of various gasoline fuels, leading to the publication of "Fuels for Advanced Combustion Engines (FACE)", which clearly defined composition and properties [2]. Studies of [3, 4], using the detailed hydrocarbon analysis (DHA), led to multi-component surrogates which matched the ignition characteristics of two of these fuels (FACE A and FACE C).

To achieve high-fidelity predictive modelling of the processes in IC gasoline fuel engines, however, the analysis of heating and evaporation characteristics of the liquid fuel droplets needs to be performed alongside the ignition analysis. The issue is becoming particularly important as modern gasoline engine designs increasingly employ direct injection strategies to achieve higher efficiencies. The main objective of the present study is to provide a general framework of *physical* surrogate fuels that represent the heating and evaporation characteristics of gasoline fuel droplets; our analysis will be focused on FACE A fuel droplets.

Heating and evaporation of liquid fuel droplets have long been studied in the context of IC engines [1]. For actual spray applications, accurate descriptions of the phenomena are further complicated by a number of other physical processes, including droplet break-up, collision, interaction with gas-phase vapour/air, and chemical reactions [5]. As the first step in modelling such complex processes, the present study is focused on the physical behaviour of a single

droplet. The effective thermal conductivity/effective diffusivity (ETC/ED) model is used in this study as a reasonable compromise between simplicity, accuracy and computational efficiency [6].

For a small number of components, the discrete component models (DCM) have been employed to capture heating and evaporation characteristics of individual components [7-20]. For a larger number of components, the most efficient approach to the modelling of droplet heating and evaporation was based on the quasi-descrete model [21-23] and multi-dimensional quasi-discrete model [24, 25].

A brief description of the model used in our analysis is presented in Section 2. The validation of the model against measurements of n-decane/n-heptane droplet surface temperatures and radii is presented in Section 3. The application of the model to the analysis of heating and evaporation of FACE A gasoline fuel and its surrogates is described in Section 4. The main results of the paper are summarised in Section 5.

2. FACE A fuel and its surrogates

A detailed analysis of hydrocarbons [3] in two alkane-rich FACE fuels, namely A and C, showed that both fuels contain n-paraffins, iso-paraffins, aromatics, naphthenes and olefins. The present study focuses on FACE A gasoline fuel with the following mass fractions of components: 10.57% n-paraffins, 86.12% iso-paraffins, 0.37% aromatics, 2.49% naphthenes and 0.45% olefins (see Table 1). Sixty-six components of this fuel are reduced to 19 components (see Table 1). The reduction in the number of components is based on replacing components within the same group and having the same chemical formulae (isomers) with the representative components having the largest initial mass fractions. The components within each group have

close thermophysical and transport properties. For example, FACE A contains 13 iso-octane isomers; the 2,2,4 trimethyl pentane (iso-octane) is chosen to represent all of them (its mass fraction is 28.56% and the total mass fraction of iso-octane isomers is 46.87%). In contrast to previous studies [22, 26] which assumed that gasoline fuel consists of n-paraffins only, the present study takes into account the contributions of other components of FACE A gasoline fuel. Our study is focused on the evaporation characteristics of the droplets of this fuel and its surrogates. The surrogates suggested so far include the five component surrogate proposed by Sarathy et al. [3] that matches the ignition delay time of the FACE A gasoline fuel, the primary reference fuel (PRF84) surrogate that matches the research octane number (RON) of FACE A gasoline fuel, and two surrogates suggested by Ahmed et al. [27]. One of the latter surrogates matches the hydrogen-to-carbon ratio H/C, RON, density and distillation curve of FACE A gasoline fuel, while the other one matches the RON of this fuel based on mole fraction linear blending.

3. Models

The analysis of heating and evaporation processes of FACE A gasoline fuel and surrogate droplets is based on the simplified model for heating and evaporation of multi-component droplets, described by Sazhin et al. [13]. The model accounts for the effects of finite liquid thermal conductivity, species diffusivities and recirculation inside droplets. Some key features of this model are described below.

3.1. Transient droplet heating

The transient heat conduction equation inside a spherically-symmetric droplet can be presented as [6]:

$$\frac{\partial T}{\partial t} = \alpha_l \left(\frac{\partial^2 T}{\partial R^2} + \frac{2}{R}\frac{\partial T}{\partial R}\right), \quad (1)$$

where $\alpha_l = \frac{k_l}{c_l \rho_l}$ is the thermal diffusivity, k_l, c_l and ρ_l are the thermal conductivity, specific heat capacity and density of the liquid, respectively, R is the distance from the centre of the droplet and t is time. In the case of moving droplets, the liquid thermal conductivity is replaced by the effective thermal conductivity $k_{\text{eff}} = \chi_T k_l$, where $\chi_T = 1.86 + 0.86\tanh\left[2.225\log_{10}\left(\text{Pe}_{d(l)}/30\right)\right]$ increases from 1 to 2.72 when the liquid Peclet number, $\text{Pe}_{d(l)} = \text{Re}_{d(l)}\text{Pr}_{d(l)}$, increases from 0 to infinity; this accounts for the effect of recirculation inside a moving droplet. The Prandtl number is defined as $\text{Pr}_{d(l)} = \frac{c_l \mu_l}{k_l}$, where μ_l is the liquid dynamic viscosity, while the Reynolds number is defined as $\text{Re}_{d(l)} = \frac{2\rho_l u_s R_d}{\mu_l}$, where u_s is the maximum liquid surface velocity (see Abramzon and Sirignano [28]). The liquid density, specific heat of evaporation, boiling temperature and critical temperature for individual components used in this study are inferred from Yaws [29]. The liquid thermal conductivity, viscosity, and heat capacity are taken from [30, 31]. The average properties of the liquid mixture are calculated based on mixing rules as described by Sazhin et al. [32].

3.2. Liquid species diffusion

For a multi-component droplet, diffusion of individual liquid components needs to be described. In the infinite diffusivity (ID) model it is assumed that the composition within the droplet is uniform at all times. In the present study the effective diffusivity (ED) model, as described below, is mainly used. The species mass fractions equation inside a spherically-symmetric droplet can be presented as [6]:

$$\frac{\partial Y_{li}}{\partial t} = D_l \left(\frac{\partial^2 Y_{li}}{\partial R^2} + \frac{2}{R}\frac{\partial Y_{li}}{\partial R}\right), \quad (2)$$

where $i \geq 1$, Y_{li} is the liquid mass fraction of species i , and D_l is the liquid mass diffusivity (see Sazhin et al. [24]). The analytical solution to Eq. (2) is given in Sazhin et al. [13]. The effect of recirculation in the moving droplet is taken into account by replacing D_l with $D_{\text{eff}} = \chi_Y D_l$, where $\chi_Y = 1.86 + 0.86\tanh\left[2.225\log_{10}\left(\text{Re}_{d(l)}\text{Sc}_{d(l)}/30\right)\right]$ increases from 1 to 2.72 when $\text{Re}_{d(l)}\text{Sc}_{d(l)}$ increases from 0 to infinity. The Schmidt number is defined as $\text{Sc}_{d(l)} = \frac{\mu_l}{\rho_l D_l}$. The combined ETC/ED model is used to account for thermal and species diffusion inside the droplet. Although this model cannot adequately predict the details of the distribution of temperature and species inside the droplet, it is believed to be adequate in predicting the average surface temperatures and mass fractions and the evaporation characteristics. It is assumed that Rault's law is valid and the vapour mole fraction at the droplet surface can be calculated as $X_{vis} = X_{lis}\, P_{i,sat}/P_{\text{amb}}$, P_{amb} is the ambient air pressure and $P_{i,sat}$ is the saturation pressure for species i (see Yaws, [33]). The liquid mole fraction at the droplet surface for species i is calculated as:$X_{lis} = \frac{Y_{lis}/M_i}{\sum_i (Y_{lis}/M_i)}$, where M_i is the molar mass of species i and Y_{lis} are the liquid mass fractions at the droplet's surface.

4. Validation of the model

The model used in the current study was previously validated against the measurements of the average droplet temperatures and radii during the cooling/heating and evaporation of ethanol/acetone and n-decane/3-pentanone droplets [13, 34]. In both cases, the full evaporation of the droplets was not observed, and the comparison was focused on the early stage of droplet cooling and heating. In this section, a new validation of the model is presented by comparing the calculated values of droplet surface temperatures and radii with experimental measurements for an n-heptane/n-decane droplet as reported by Daif et al. [35]. The experiments were carried out

for suspended droplets in a wind tunnel; the droplet surface temperatures were measured by a thermographic infrared system and droplet diameters by a CCD camera. The initial conditions were the following: the initial droplet radius was 743 μm, with mass fractions of 21.2% n-heptane/78.8% n-decane, the initial droplet temperature was 294 K, ambient temperature was 348 K, ambient pressure was 1.0 atm and droplet relative velocity was 3.1 m/s. The results of the comparison are shown in Fig. 1. The first 12 s refer to the time before opening the damper to allow air to move over a droplet after its successful suspension.

As one can see from Fig. 1, the ETC/ED model predicts values of both surface temperatures and droplet radii squared which are close to those inferred from the experimental measurements with average relative errors less than 0.9% and 5.0%, respectively. These errors increased to 2% and 14% when the ITC/ID model was used. The maximal error in temperature measurements was shown to be ±2.0%, and the error in droplet diameter measurements for a 1.0 mm diameter droplet was shown to be 3%. This error increases with time [35]. The surface temperature predicted by the ETC/ED model is lower compared to that predicted by the ITC/ID model, which is attributed to fast evaporation of n-heptane (lighter component) from the droplet surface in the case of the ETC/ED model, while in the ITC/ID model the heat which reaches the droplet is used for the heating of the entire droplet causing a lower evaporation rate of n-heptane. These results demonstrate the importance of consideration of the transport processes inside the droplet for accurate prediction of the heating and evaporation characteristics. Note that the effect of thermal swelling, due to density change with temperature, on droplet radius was also taken into account.

5. Application to modelling of droplets of FACE A gasoline fuel and its surrogates

Firstly, the analysis of this section is focused on the FACE A gasoline fuel and four surrogates: PRF84, a five component surrogate chosen for its ability to match the ignition delay time of the FACE A gasoline fuel [3], and two additional surrogates suggested by Ahmed et al. [27]. Table 2 summarises the mole fractions of the above-mentioned four surrogates, which are referred to as PRF84, Surr1, Surr2 and Surr3. All these surrogates for FACE A consist of n-paraffins and iso-paraffins only, and ignore more than 3% of aromatics, naphthenes and olefins that are present in FACE A gasoline fuel. Note that the evaporation characteristics were not used in developing these surrogates.

Figure 2 shows the predicted droplet surface temperatures and radii versus time for FACE A and four surrogates shown in Table 2. The ETC/ED model was used with the initial droplet radius and temperature equal to 10 μm and 300 K, respectively. The ambient air temperature and pressure were taken equal to 450 K and 0.3 MPa, respectively, while the relative velocity was set at 10 m/s. All ambient conditions were assumed to be constant, and the effect of droplets on ambient air was ignored. As one can see from Figure 2, the evaporation time of a FACE A droplet is approximately 10% longer than that of the four surrogate fuel droplets. This is attributed to a larger amount of heavier components in the FACE A fuel. The droplet lifetimes predicted for the four surrogate fuel droplets are very close except that the evaporation time of the PRF84 droplet is slightly longer than that of the other three surrogate droplets. This is related to the fact that PRF84 contains only n-heptane and iso-octane while other surrogates contain lighter components such as n-butane, iso-pentane and 2-methyl hexane. At an early stage of the droplet evaporation, the predicted droplet surface temperatures for the FACE A droplet are lower than those for the four surrogates and the PRF84 droplet yields the highest surface temperature.

This is attributed to the contribution of light components in FACE A. After the initial heating-up period, the predicted surface temperatures of all four surrogate fuel droplets reach the wet bulb temperature and stay constant, while for the FACE A fuel droplet the temperature increases until it fully evaporates. This is attributed to the second heat-up period for the heaviest component in the FACE A droplet.

Figure 3 shows the liquid mass fractions of the FACE A components at the surface of the droplet versus time for the same conditions as in Fig. 2. The numbering of individual components is the same as in Table 1. As one can see in Fig. 3, the mass fractions of light components, such as n-butane (1), iso-pentane (2) and 2-methylpentane (4), monotonically decrease with time, while the mass fraction of the heaviest component, 1-methyl-2-propylcyclohexane (16), monotonically increases with time. Intermediate components show more complex behaviour; their mass fractions initially increase with time and then decrease.

As follows from the analysis presented above, none of the four surrogate fuels can lead to accurate prediction of the evaporation characteristics of the 19-component FACE A fuel droplets. This is an expected result remembering that these surrogates were developed without considering the evaporation characteristics as a target metric. Therefore, three additional surrogate fuels, referred to as *physical surrogates*, are proposed in this study. Firstly, an 8-component surrogate, Surr4, retaining the same mass fractions of n-butane, n-heptane, iso-pentane, and iso-octane as in FACE A, is suggested. These components contribute more than 70% of the total mass of FACE A gasoline fuel. Components (4-6), 2-methylpentane, 3-methylhexane and 2,3-dimethylpentane, show similar evaporation behaviour (see Fig. 3); they are replaced by 3-methylhexane which contributes 25.87% of FACE A. Also, components 8-11 and 18 have similar evaporation characteristics; these are replaced by 2,6-dimethyloctane (9).

178 Furthermore, the groups of components (12-15) and (16, 17 and 19) are replaced by components
179 14 and 16, respectively.

180 The above-mentioned composition is further simplified in a 7-component surrogate, Surr5,
181 in which n-heptane and a representative of components 12-15 (1t,2-dimethylcyclopentnane) are
182 replaced by n-heptane. Finally a 6-component surrogate, Surr6, is suggested. In this surrogate
183 iso-octane and a representative of components 8-11 and 18 (2,6-dimethyloctane) are replaced
184 with iso-octane. The mass fractions of the components of the above-mentioned three new
185 physical surrogates, Surr4, Surr5 and Surr6, are given in Table 3.

186 A comparison between the droplet surface temperatures and radii predicted for FACE A
187 fuel, Surr4, Surr5 and Surr6 is shown in Fig. 4. Comparing the results shown in Fig. 4 with those
188 shown in Fig. 2, one can see that all physical surrogate fuels lead to more accurate predictions of
189 droplet surface temperatures and radii than the previously suggested surrogates. The evaporation
190 time predicted for the Surr6 droplet is almost identical to that of the FACE A fuel droplet, while
191 the maximal error in the prediction of the droplet surface temperature does not exceed 2%, which
192 is acceptable in most engineering applications. The evaporation times predicted for Surr4 and
193 Surr5 droplets are longer than those of the FACE A droplets by 5%. The difference between the
194 droplet surface temperatures predicted for the Surr4 and Surr5 and that for FACE A does not
195 exceed 13%. Surr5 is selected as an optimal physical surrogate in our study.

196 To further illustrate the ability of the new surrogates to represent FACE A fuel in engine
197 applications, three additional target properties are considered: the H/C ratio, molecular weight,
198 and RON. Matching molar masses and H/C ratios of the target fuels indicates matching of both
199 diffusivity and flame speed [36] while matching RON indicates matching of the ignition delay
200 time [3]. Table 4 shows the values of these three properties for FACE A fuel and 7 surrogates

used in our study. The values of these properties for FACE A, PRF84, Surr1, 2 and 3 are taken from Sarathy et al. [3] and Ahmed et al. [27]. The RONs for Surr4, 5 and 6 are calculated following the procedure suggested by Ghosh et al. [37] based on the detailed composition of fuel. As can be seen from this table, compared with the previously suggested surrogates, the physical surrogates proposed in our study have values of RON, molar masses, and H/C ratios which are marginally closer to those of FACE A fuel. Therefore, the new physical surrogates have not only improved evaporation prediction, but also have better representations of other important physical and chemical characteristics of FACE A fuel.

Figure 5(a) shows the time evolution of droplet surface, average and centre temperatures (T_s, T_{av} and T_c) predicted by the ETC/ED model for the Surr5 droplet for the same conditions as used in Figs. 2-4. The average temperature is calculated following Sazhin [38]. As one can see from this figure, all three temperatures are well separated during the first heat-up period; at the later time instants these temperatures tend to merge (the droplet becomes well mixed). The difference between these temperatures cannot be ignored as it affects the break-up and collision processes when the model is applied to fuel sprays. The effect of heating and evaporation models of mono-component droplets on spray penetration was studied in [39], where it was demonstrated that the dependence of the spray penetration length on heating and evaporation models can be strong. The temperature distribution inside a Surr5 droplet, predicted by the ETC/ED model, is shown in Fig. 5(b) at five time instants. The values of surface temperatures inferred from this figure are the same as shown in Fig. 5(a). Note that, at the time instant 1.0 ms, the temperature distribution inside the droplet is nearly uniform.

Figure 6(a) shows the time evolution of the liquid mass fractions of components of Surr5 at the surface of the droplets for the same conditions as in Figs. 2-5. The mass fractions of n-butane

(1) and iso-pentane (3) monotonically decrease, while the mass fractions of n-heptane (3), 3-methylhexane (5) and iso-octane (7) firstly slightly increase with time and then rapidly decrease after about 60% of the droplet lifetime. The mass fraction of 2, 6-dimethyloctane (9) increases with time and reaches its peak when the mass fractions of (3), (5) and (7) are almost zero, and then it starts to decrease. The mass fraction of 1-methyl-2-propylcyclohexane (16) monotonically increases with time. These results are in good agreement with the conclusions drawn from the analysis of the results shown in Fig. 3.

The distributions of mass fractions of components of Surr5 inside the droplet at various instants of time are shown in Figs. 6(b)-(d). The results are consistent with those shown in Fig. 6(a). The distribution of mass fractions of all components presented in these figures indicates that the models based on zero or infinitely large diffusivities inside droplets cannot accurately describe the evaporation of droplets under these conditions.

6. Conclusions

The previously developed discrete component model for heating and evaporation of multi-component fuel droplets, taking into account the effects of finite thermal conductivity, species diffusivity and recirculation inside droplets, was applied to the analysis of heating and evaporation of droplets of FACE A gasoline fuel and its surrogates. The model was initially validated against measurements for n-heptane/n-decane mixture droplet surface temperatures and radii. At the next stage, the model was applied to analysis of heating and evaporation of droplets of four surrogates of FACE A identified from the literature. It was shown that for these surrogates there were significant differences in the predicted droplet surface temperatures and radii compared with those predicted for the FACE A fuel droplets. Then three new ‘physical’

surrogates were proposed and their predictions of droplet surface temperatures and radii were shown to agree well with the predictions for FACE A fuel droplets. Comparisons showed that H/C, molar mass and RON for each of the new surrogates were in good agreement with those of FACE A fuel. It is concluded that FACE A gasoline fuel can be accurately represented by the suggested 7 component surrogates when describing both heat/mass transfer and ignition/combustion processes.

Acknowledgements

Research reported in this publication was supported by King Abdullah University of Science and Technology (KAUST), Saudi Aramco under the FUELCOM program and EPSRC, UK (project EP/J006793/1).

References

[1] Heywood JB. Internal combustion engine fundamentals. Mcgraw-hill New York; 1988.
[2] Pitz WJ, Cernansky NP, Dryer FL, Egolfopoulos F, Farrell J, Friend D, Pitsch H, Development of an experimental database and chemical kinetic models for surrogate gasoline fuels, in, SAE Technical Paper, 2007.
[3] Sarathy SM, Kukkadapu G, Mehl M, Wang W, Javed T, Park S, Oehlschlaeger MA, Farooq A, Pitz WJ, Sung C-J. Ignition of alkane-rich FACE gasoline fuels and their surrogate mixtures. Proceedings of the Combustion Institute 2015; 35: 249-257.
[4] Javed T, Nasir EF, Es-sebbar E-t, Farooq A. A comparative study of the oxidation characteristics of two gasoline fuels and an n-heptane/iso-octane surrogate mixture. Fuel 2015; 140: 201-208.
[5] Sazhina E, Sazhin S, Heikal M, Babushok V, Johns R. A detailed modelling of the spray ignition process in Diesel engines. Combustion Science and Technology 2000; 160: 317-344.
[6] Sazhin S. Droplets and sprays. Springer; 2014.
[7] Abraham J, Magi V, A model for multicomponent droplet vaporization in sprays, in, SAE Technical Paper, 1998.
[8] Aggarwal S, Mongia H. Multicomponent and high-pressure effects on droplet vaporization. Journal of engineering for gas turbines and power 2002; 124: 248-255.
[9] Brenn G, Deviprasath L, Durst F, Fink C. Evaporation of acoustically levitated multi-component liquid droplets. International Journal of Heat and Mass Transfer 2007; 50: 5073-5086.
[10] Sirignano WA, Wu G. Multicomponent-liquid–fuel vaporization with complex configuration. International Journal of Heat and Mass Transfer 2008; 51: 4759-4774.

[11] Ghosh J, Mukhopadhyay A, Rao GV, Sanyal D. Analysis of evaporation of dense cluster of bicomponent fuel droplets in a spray using a spherical cell model. International Journal of Thermal Sciences 2008; 47: 584-590.
[12] Maqua C, Castanet G, Lemoine F. Bicomponent droplets evaporation: Temperature measurements and modelling. Fuel 2008; 87: 2932-2942.
[13] Sazhin S, Elwardany A, Krutitskii P, Castanet G, Lemoine F, Sazhina E, Heikal M. A simplified model for bi-component droplet heating and evaporation. International Journal of Heat and Mass Transfer 2010; 53: 4495-4505.
[14] Sazhin S, Elwardany A, Krutitskii P, Deprédurand V, Castanet G, Lemoine F, Sazhina E, Heikal M. Multi-component droplet heating and evaporation: numerical simulation versus experimental data. International Journal of Thermal Sciences 2011; 50: 1164-1180.
[15] Strotos G, Gavaises M, Theodorakakos A, Bergeles G. Numerical investigation of the evaporation of two-component droplets. Fuel 2011; 90: 1492-1507.
[16] Abianeh OS, Chen C. A discrete multicomponent fuel evaporation model with liquid turbulence effects. International Journal of Heat and Mass Transfer 2012; 55: 6897-6907.
[17] Saha K, Abu-Ramadan E, Li X. Multicomponent evaporation model for pure and blended biodiesel droplets in high temperature convective environment. Applied Energy 2012; 93: 71-79.
[18] Dgheim J, Abdallah M, Nasr N. Evaporation phenomenon past a rotating hydrocarbon droplet of ternary components. International Journal of Heat and Fluid Flow 2013; 42: 224-235.
[19] Gopireddy S, Gutheil E. Numerical simulation of evaporation and drying of a bi-component droplet. International Journal of Heat and Mass Transfer 2013; 66: 404-411.
[20] Yasin MM, Cant R, Chong C, Hochgreb S. Discrete multicomponent model for biodiesel spray combustion simulation. Fuel 2014; 126: 44-54.
[21] Sazhin S, Elwardany A, Sazhina E, Heikal M. A quasi-discrete model for heating and evaporation of complex multicomponent hydrocarbon fuel droplets. International Journal of Heat and Mass Transfer 2011; 54: 4325-4332.
[22] Elwardany A, Sazhin S. A quasi-discrete model for droplet heating and evaporation: Application to Diesel and gasoline fuels. Fuel 2012; 97: 685-694.
[23] Elwardany A, Sazhin S, Farooq A. Modelling of heating and evaporation of gasoline fuel droplets: a comparative analysis of approximations. Fuel 2013; 111: 643-647.
[24] Sazhin S, Al Qubeissi M, Nasiri R, Gun'ko V, Elwardany A, Lemoine F, Grisch F, Heikal M. A multi-dimensional quasi-discrete model for the analysis of Diesel fuel droplet heating and evaporation. Fuel 2014; 129: 238-266.
[25] Al Qubeissi M, Sazhin S, Turner J, Begg S, Crua C, Heikal M. Modelling of gasoline fuel droplets heating and evaporation. Fuel 2015.
[26] Arias-Zugasti M, Rosner DE. Multicomponent fuel droplet vaporization and combustion using spectral theory for a continuous mixture. Combustion and Flame 2003; 135: 271-284.
[27] Ahmed A, Goteng G, Shankar VS, Al-Qurashi K, Roberts WL, Sarathy SM. A computational methodology for formulating gasoline surrogate fuels with accurate physical and chemical kinetic properties. Fuel 2015; 143: 290-300.
[28] Abramzon B, Sirignano W. Droplet vaporization model for spray combustion calculations. International journal of heat and mass transfer 1989; 32: 1605-1618.
[29] Yaws CL. Thermophysical properties of chemicals and hydrocarbons. William Andrew; 2008.
[30] Yaws CL. Handbook of transport property data: viscosity, thermal conductivity, and diffusion coefficients of liquids and gases. Inst of Chemical Engineers; 1995.

[31] Yaws CL. Yaws handbook of thermodynamic properties for hydrocarbons and chemicals. 2006.
[32] Sazhin S, Al Qubeissi M, Kolodnytska R, Elwardany A, Nasiri R, Heikal M. Modelling of biodiesel fuel droplet heating and evaporation. Fuel 2014; 115: 559-572.
[33] Yaws CL. Handbook of Vapor Pressure: Organic Compounds. Gulf Professional Publishing; 1995.
[34] Elwardany A, Gusev I, Castanet G, Lemoine F, Sazhin S. Mono-and multi-component droplet cooling/heating and evaporation: comparative analysis of numerical models. Atomization and Sprays 2011; 21.
[35] Daif A, Bouaziz M, Chesneau X, Cherif AA. Comparison of multicomponent fuel droplet vaporization experiments in forced convection with the Sirignano model. Experimental thermal and fluid science 1998; 18: 282-290.
[36] Mannaa O, Mansour MS, Roberts WL, Chung SH. Laminar burning velocities at elevated pressures for gasoline and gasoline surrogates associated with RON. Combustion and Flame 2015; 162: 2311-2321.
[37] Ghosh P, Hickey KJ, Jaffe SB. Development of a detailed gasoline composition-based octane model. Industrial & engineering chemistry research 2006; 45: 337-345.
[38] Sazhin SS. Advanced models of fuel droplet heating and evaporation. Progress in energy and combustion science 2006; 32: 162-214.
[39] Abdelghaffar W, Elwardany A, Sazhin S. Modeling of the processes in diesel engine-like conditions: Effects of fuel heating and evaporation. Atomization and Sprays 2010; 20: 737-747.

Figure captions

Fig. 1 Time evolution of predicted and measured droplet surface temperatures and radii for a 21.3% n-heptane/78.8% n-decane droplet with initial homogeneous temperature of 294 K and initial radius of 743 μm in an air with constant ambient pressure and temperature of 0.1 MPa and 345 K, respectively. The relative droplet velocity is 3.1 m/s.

Fig. 2 Time evolution of the surface temperatures and radii predicted by the ETC/ED model for FACE A, PRF84, Surr1, Surr2, and Surr3 fuel droplets; the gas temperature and pressure are assumed to be constant and equal to 450 K and 0.3 MPa, respectively; the relative droplet velocity is assumed to be constant and equal to 10 m/s; the initial droplet radius and homogeneous temperature are assumed to be equal to 10 μm and 300 K, respectively.

Fig. 3 The liquid mass fractions of components of FACE A gasoline fuel at the droplet surface versus time for the same conditions as in Fig. 2.

Fig. 4 Droplet surface temperatures and radii versus time calculated under the assumption that the fuels used are FACE A, and surrogates Surr4, Surr5 and Surr6. The values of other input parameters are the same as in Figs. 2-3.

Fig. 5 (a) Time evolution of droplet surface, average and centre temperatures (T_s, T_{av} and T_c) for Surr5 for the same conditions as in Figs. 2-4; (b) temperature distributions as functions of the normalised radius $r = R/R_d$ for the same conditions as in Fig. 5a.

Fig. 6 (a) Liquid mass fractions at the droplet surface for the components of Surr5 versus time predicted by the ETC/ED model for the same conditions as in Figs. 2-5; (b)-(d) Mass fractions of components of Surr5 versus normalised distance from the droplet centre, predicted by the ETC/ED model for the same conditions as in Figs. 2-5, at three instants of time.

Table captions

Table 1 Mass fractions, molecular weights, boiling and critical temperatures of the components of FACE A gasoline fuel.

Table 2. Mole fractions of four surrogates of FACE A gasoline fuel.

Table 3. Mass fractions (in %) of three new 'physical' surrogates of FACE A gasoline fuel.

Table 4. H/C ratio, molecular weight and RON of FACE A fuel and seven surrogates.

Table

Table 1 Mass fractions, molecular weights, boiling and critical temperatures of the components of FACE A gasoline fuel.

Group	#	Name	Formula	Mass fraction	MW [kg/kmol]	T_b [K]	T_{cr} [K]
N-paraffins	1	n-butane	n-C_4H_{10}	0.0392	58.0	272.65	425.12
	2	n-heptane	n-C_7H_{16}	0.0665	100.0	371.58	540.20
Iso-paraffins	3	iso-pentane	C_5H_{12}	0.1278	72.0	300.99	460.40
	4	2-methylpentane	C_6H_{14}	0.0255	86.0	333.41	497.70
	5	3-methylhexane	C_7H_{16}	0.1158	100.0	365.00	535.20
	6	2,3-dimethylpentane	C_7H_{16}	0.1175	100.0	362.93	537.30
	7	2,2,4 trimethylpentane	C_8H_{18}	0.4687	114.0	372.39	543.80
	8	2,3,4 trimethyl hexane	C_9H_{20}	0.0022	128.0	412.20	594.50
	9	2,6-dimethyloctane	$C_{10}H_{22}$	0.0040	142.0	433.53	606.00
Aromatics	10	o-xylene	C_8H_{10}	0.0002	106.0	417.58	630.30
	11	1 methyl-2ethylbenzene	C_9H_{12}	0.0032	120.0	425.56	631.00
	12	1 mehyl-3-n-propylbenzene	$C_{10}H_{14}$	0.0003	134.0	454.95	654.00
Cyclo-alkanes	13	cyclo-pentane	C_5H_{10}	0.0004	70.0	322.40	511.70
	14	1t,2-dimethylcyclopentnane	C_7H_{14}	0.0123	98.0	370.00	556.47
	15	methyl cyclohexane	C_7H_{14}	0.0029	98.0	374.08	572.10
	16	1-methyl-2-propylcyclohexane	$C_{10}H_{20}$	0.0093	140.0	449.15	667.00
Olefins	17	hexene-1	C_6H_{12}	0.0007	84.0	336.63	504.00
	18	nonene-1	C_9H_{18}	0.0023	126.0	420.02	594.00
	19	2-methyl-2-hexene	C_7H_{14}	0.0015	98.0	368.56	546.77

Table 2. Mole fractions of four surrogates of FACE A gasoline fuel.

Component	PRF84 [3]	Surr1, [3]	Surr2, [27]	Surr3, [27]
n-butane	0.0	7.0	7.7	5.0
n-heptane	17.6	7.0	10.0	5.0
iso-pentane	0.0	15.0	12.0	5.0
2-methylhexane	0.0	11.0	10.3	15.0
iso-octane	82.4	60.0	60.0	70.0

Table 3. Mass fractions (in %) of three new 'physical' surrogates of FACE A gasoline fuel.

#	Component	Surr4 (8 Comp)	Surr5 (7 Comp)	Surr6 (6 Comp)
1	n-butane	3.919	3.919	3.919
2	n-heptane	6.652	8.238	8.238
3	iso-pentane	12.784	12.784	12.784
5	3 methyl hexane	25.875	25.875	25.875
7	iso-octane	46.869	46.869	48.063
9	2,6-dimethyloctane	1.194	1.194	0.000
14	1t,2 dimethylcyclopentane	1.585	0.000	0.000
16	1-methyl-2-propylcyclohexane	1.121	1.121	1.121

Table 4. H/C ratio, molecular weight and RON of FACE A fuel and seven surrogates.

Target	FACE A	PRF 84	Surr1	Surr2	Surr3	Surr4	Surr5	Surr6
H/C ratio	2.29	2.26	2.28	2.28	2.26	2.29	2.3	2.3
M (kg/kmol)	97.8	112	101.5	102	106.5	98.6	98.64	98.44
RON	83.5	84	85.3	86.6	85.6	80.3	79	79.5

Figure

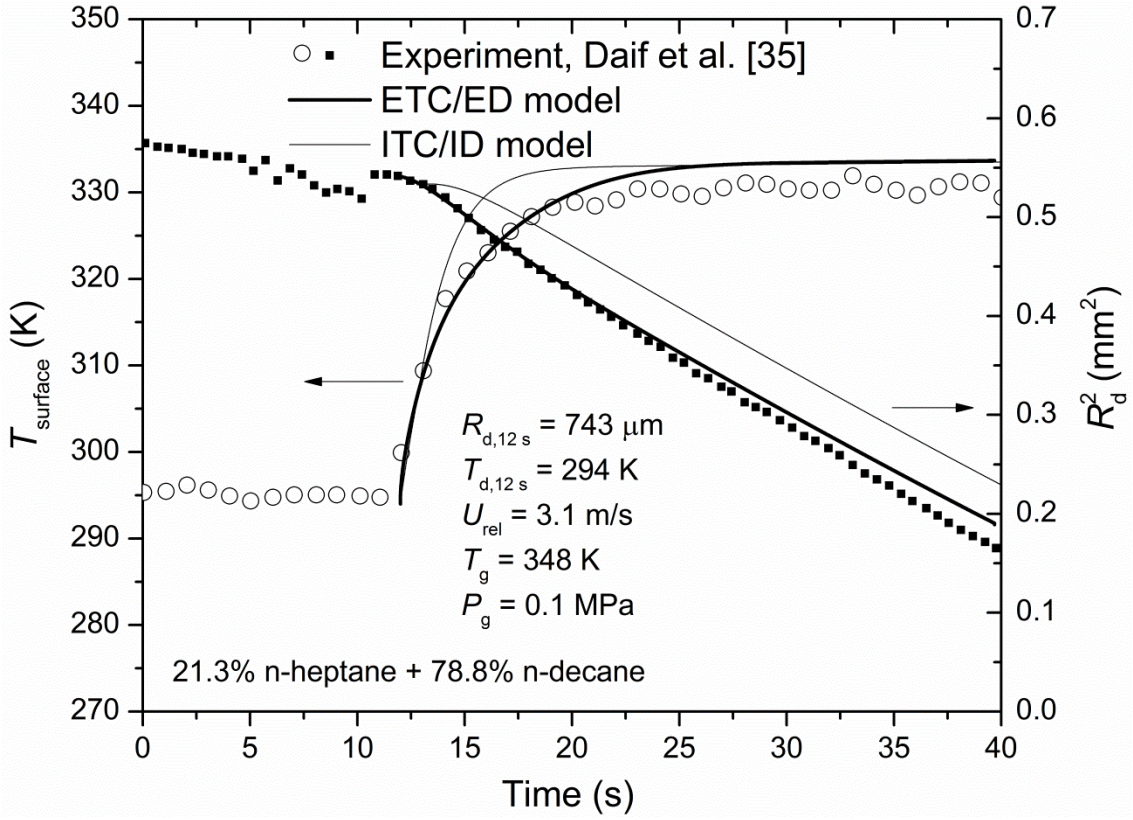
Experiment, Daif et al. [35]
ETC/ED model
ITC/ID model
$R_{d,12\,s}$ = 743 μm
$T_{d,12\,s}$ = 294 K
U_{rel} = 3.1 m/s
T_g = 348 K
P_g = 0.1 MPa
21.3% n-heptane + 78.8% n-decane
$T_{surface}$ (K)
R_d^2 (mm^2)
Time (s)
350
340
330
320
310
300
290
280
270
0.7
0.6
0.5
0.4
0.3
0.2
0.1
0.0
0
5
10
15
20
25
30
35
40

Fig. 1

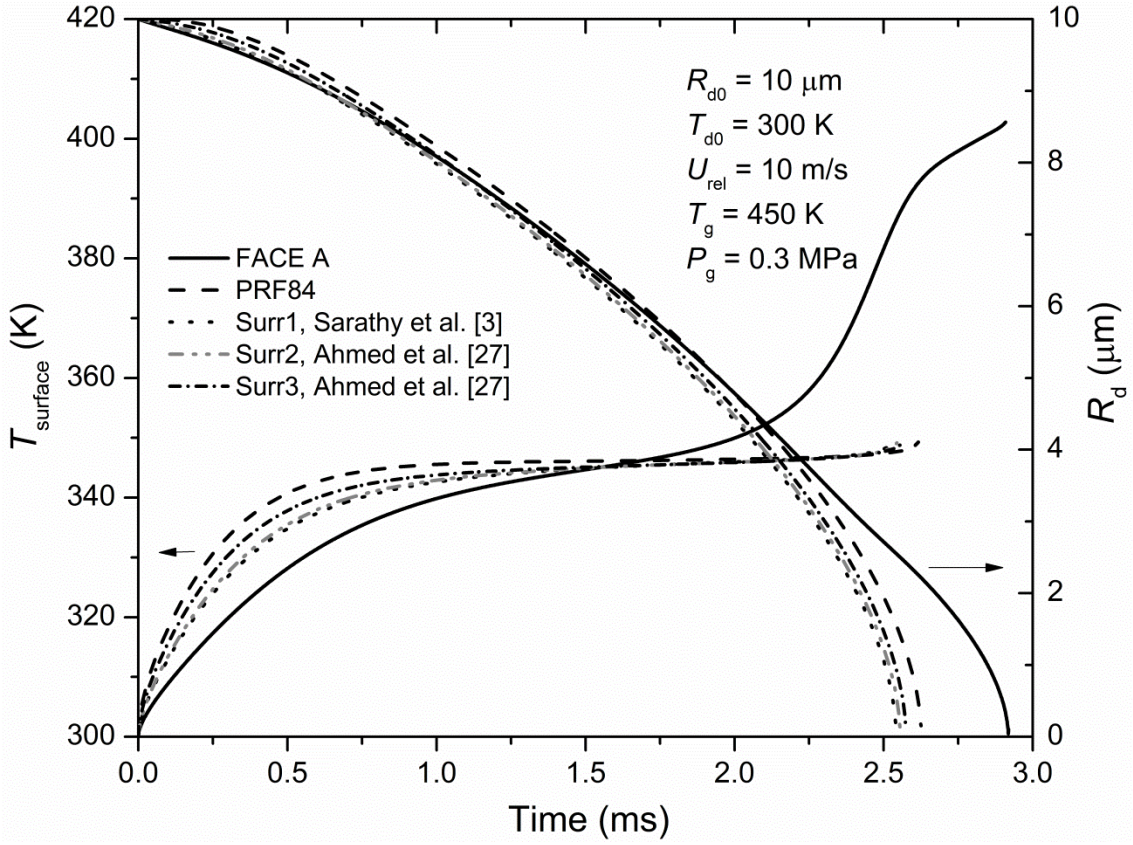
R_{d0} = 10 μm
T_{d0} = 300 K
U_{rel} = 10 m/s
T_g = 450 K
P_g = 0.3 MPa
FACE A
PRF84
Surr1, Sarathy et al. [3]
Surr2, Ahmed et al. [27]
Surr3, Ahmed et al. [27]
$T_{surface}$ (K)
R_d (μm)
Time (ms)
420
400
380
360
340
320
300
10
8
6
4
2
0
0.0
0.5
1.0
1.5
2.0
2.5
3.0

Fig. 2

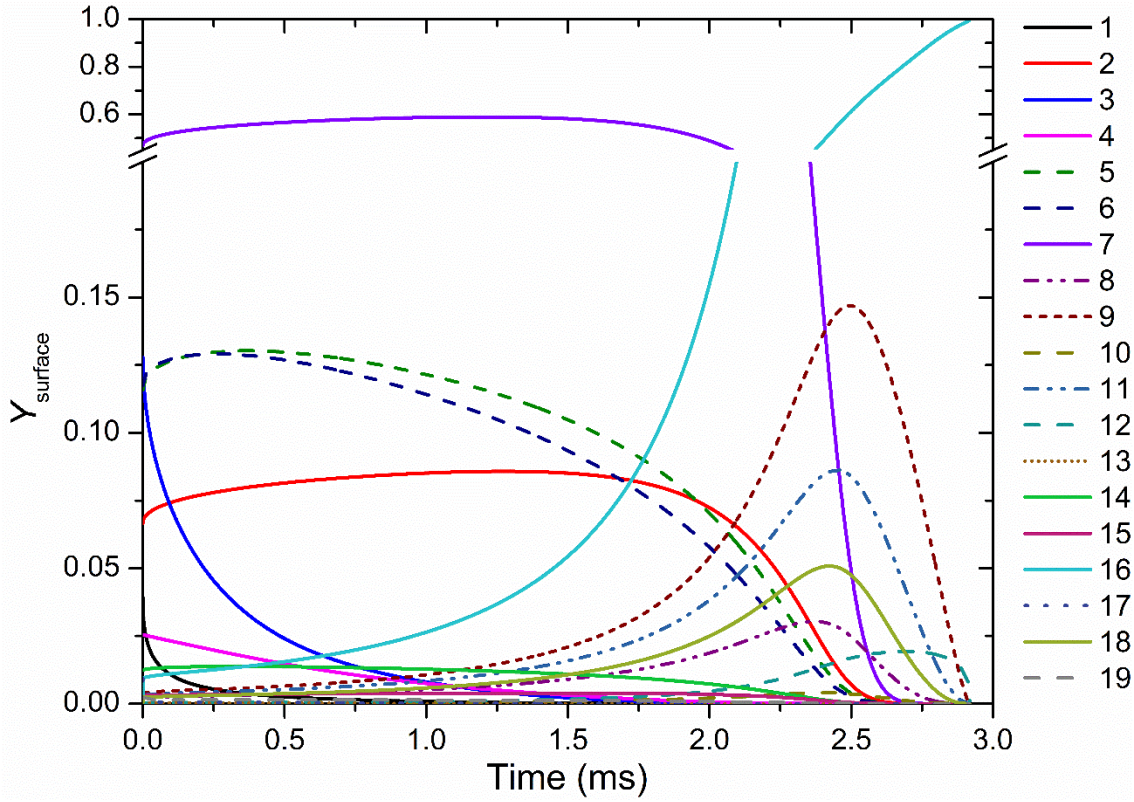
1.0
0.8
0.6
0.15
0.10
0.05
0.00
Y surface
0.0
0.5
1.0
1.5
2.0
2.5
3.0
Time (ms)
1
2
3
4
5
6
7
8
9
10
11
12
13
14
15
16
17
18
19

Fig. 3

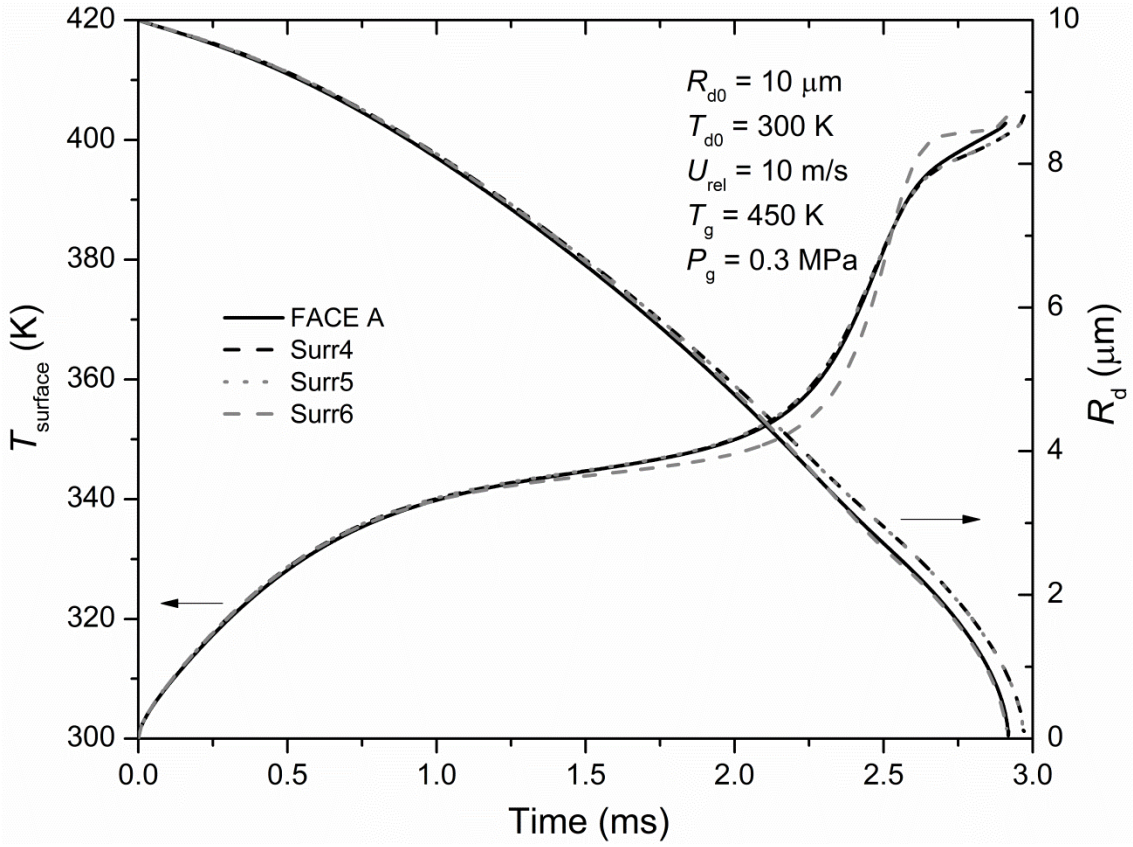
R_{d0} = 10 μm
T_{d0} = 300 K
U_{rel} = 10 m/s
T_g = 450 K
P_g = 0.3 MPa
FACE A
Surr4
Surr5
Surr6
$T_{surface}$ (K)
R_d (μm)
Time (ms)
420
400
380
360
340
320
300
10
8
6
4
2
0
0.0
0.5
1.0
1.5
2.0
2.5
3.0

Fig. 4

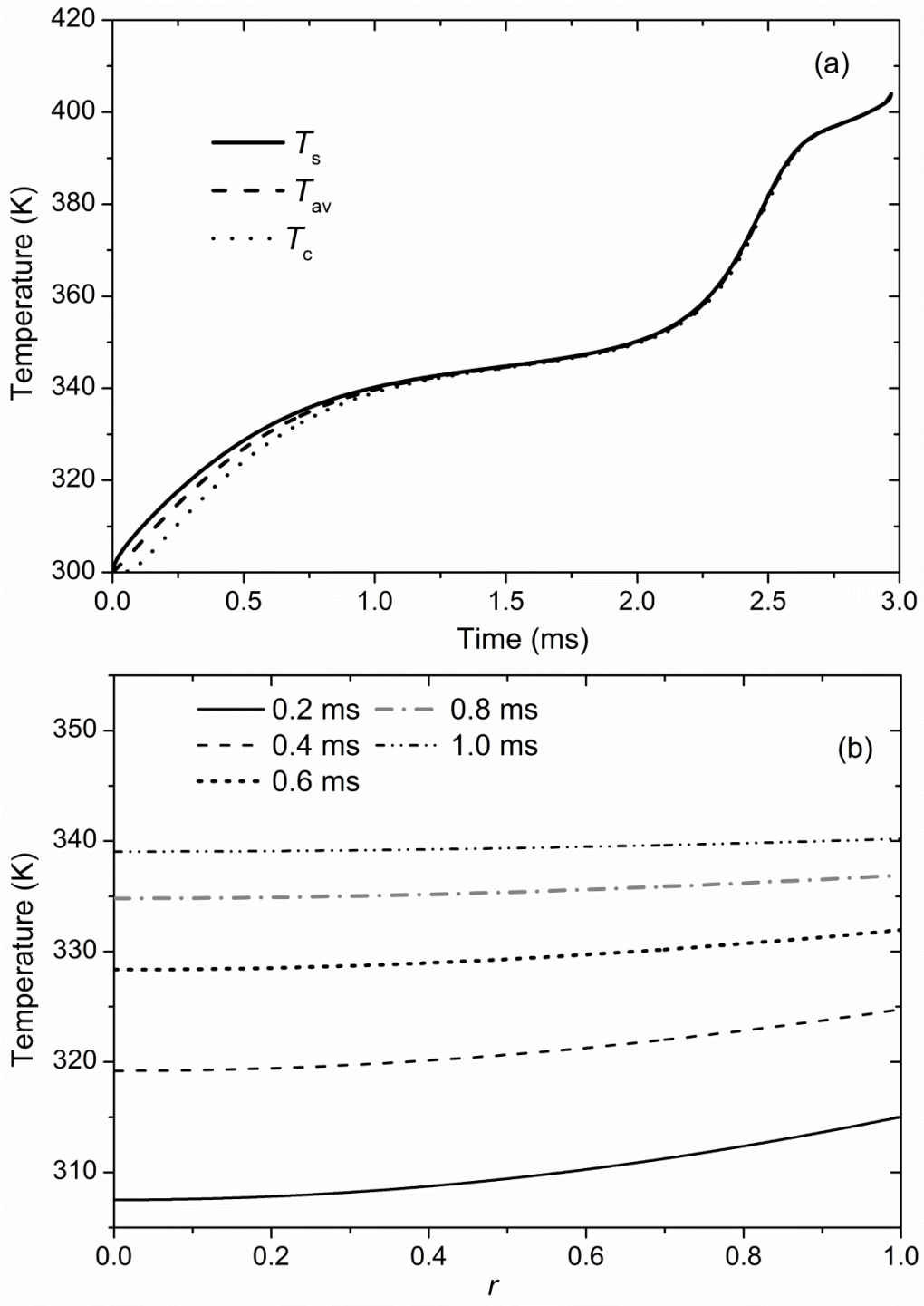
(a)
T_s
T_{av}
T_c
Temperature (K)
Time (ms)
420
400
380
360
340
320
300
0.0
0.5
1.0
1.5
2.0
2.5
3.0
(b)
0.2 ms
0.4 ms
0.6 ms
0.8 ms
1.0 ms
Temperature (K)
r
350
340
330
320
310
0.0
0.2
0.4
0.6
0.8
1.0

Fig. 5

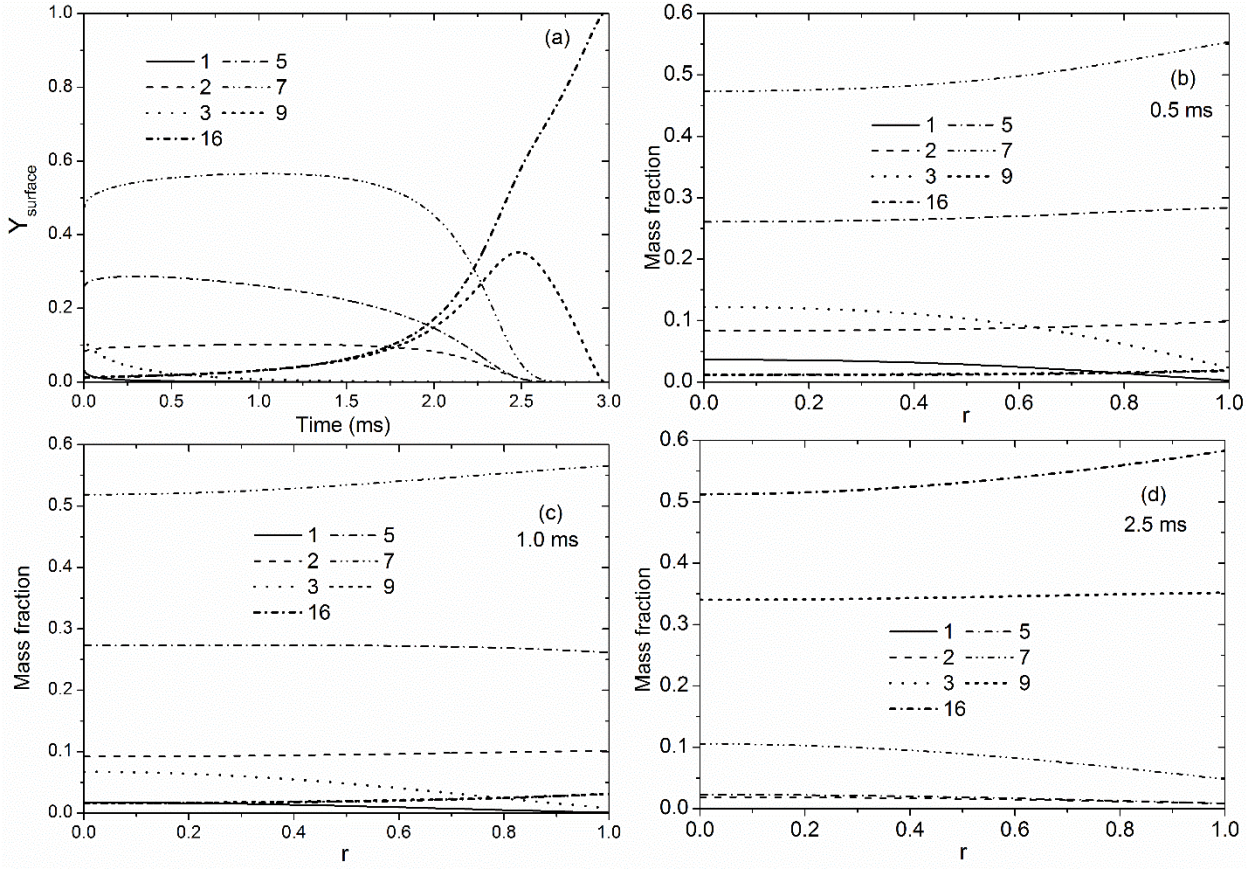
(a)
1
2
3
16
5
7
9
$Y_{surface}$
Time (ms)
(b)
0.5 ms
Mass fraction
r
(c)
1.0 ms
(d)
2.5 ms

Fig. 6